

Acne Treatment With a 1,450 nm Wavelength Laser and Cryogen Spray Cooling

Dilip Y. Paithankar, PhD,^{1*} E. Victor Ross, MD,² Bilal A. Saleh, MEng,¹ Mark A. Blair, MD,² and Bradley S. Graham, MD²

¹Candela Corporation, 530 Boston Post Road, Wayland, Massachusetts

²Naval Medical Center, San Diego, 34520 Bob Wilson Drive, San Diego, California

Background and Objectives: A laser with a wavelength in the mid-IR range targeting the depth in skin where sebaceous glands are located in combination with cryogen spray cooling was evaluated for treatment of acne. In this non-ablative treatment, the laser energy heats the dermal volume encompassing sebaceous glands whereas the cold cryogen spray preserves the epidermis from thermal damage.

Study Design/Materials and Methods: Monte Carlo simulations and heat transfer calculations were performed to optimize the heating and cooling parameters. A variety of heating and cooling parameters were tested in an *in vivo* rabbit ear study to evaluate the histological effect of the device on sebaceous glands and skin. Similar experiments were performed on *ex vivo* human skin. A clinical study for the treatment of acne on backs of human males was also conducted.

Results: Monte Carlo simulations and heat transfer calculations resulted in a thermal damage profile that showed epidermal preservation and peak damage in the upper dermis where sebaceous glands are located. *Ex vivo* human skin histology confirmed the damage profile qualitatively. *In vivo* rabbit ear histology studies indicated short-term thermal alteration of sebaceous glands with epidermal preservation. In the human clinical study on the back, a statistically significant reduction in lesion count on the treated side compared to the control side was seen ($p < 0.001$). Side effects were transient and few.

Conclusions: The studies reported here demonstrate the feasibility of treating acne using a photothermal approach with a mid-IR laser and cryogen cooling. *Lasers Surg. Med.* 31:106–114, 2002. © 2002 Wiley-Liss, Inc.

Key words: cryogen cooling; laser treatment of acne; Monte Carlo light transport modeling; non-ablative; sebaceous glands

INTRODUCTION

Acne vulgaris is the most common skin disease in the United States, and accounts for 25% of all visits to dermatologists [1]. While the highest incidence of acne occurs between the ages of 15 and 18 years in both males and females, acne can begin at virtually any age and occasionally persist into adulthood. Because it most commonly affects the face and can lead to permanent scarring, acne

can have profound and long-lasting psychological effects. Pustules and scarring occur at an age when the potential impact on the patient is greatest. Acne appears to have the potential to damage, perhaps even in the long term, the emotional well-being of patients [2].

Acne is a disease of the pilosebaceous unit of the skin wherein there is an inflammatory reaction in the oil-producing follicle [3]. The basic lesion of acne is the comedo, an enlargement of the sebaceous follicle. The formation of the comedo begins with defective keratinization of the follicular duct, resulting in abnormally adherent epithelial cells and plugging of the duct with sebum and keratinous debris. When the lipid egress is blocked and the plug pushes up to the surface, it causes a blackhead (or open comedo). When the opening is very tightly closed, the material behind it causes a whitehead (or closed comedo). Some comedones evolve into inflammatory papules, pustules, nodules, or chronic granulomatous lesions. Proliferation of *Propionibacterium acnes* (*P. acnes*) results in the production of inflammatory compounds resulting in neutrophil chemotaxis [2].

Acne patients routinely receive years of topical or systemic therapies. Current treatment options include topical anti-inflammatory, topical peeling agents, topical and oral antibiotics, topical and oral retinoids, and hormonal agonists and antagonists. These treatments must be used over long periods of time and are associated with several potential side effects. Pervasive use of antibiotics can lead to the emergence of resistance in *P. acnes* [4]. Systemic isotretinoin has been successfully used to treat acne. However, it has extraordinary teratogenicity and is linked with side effects that include dry mouth and skin, itching, dermatitis, eye irritation, and hepatotoxicity [5]. Most of these therapies are expensive and associated with at least mild systemic or localized side effects [1]. With the exception of systemic isotretinoin, traditional acne remedies do not alter the sebaceous glands from which acne lesions originate

Grant sponsor: National Institutes of Health; Grant number: 1R43AR46938-01.

*Correspondence to: Dilip Y. Paithankar, Candela Corporation, 530 Boston Post Road, Wayland, MA 01778.

E-mail: dilip.paithankar@c1zr1.com

Accepted 13 May 2002

Published online in Wiley InterScience

(www.interscience.wiley.com).

DOI 10.1002/lsm.10086

and the remedies remain non-curative. For many patients, however, acne tends to spontaneously involute after adolescence. This phenomenon is not well understood [6]. A successful treatment, systemic isotretinoin is associated with shrinking of sebaceous glands and a remarkable reduction in sebum output during treatment [6]. However, 1 year after cessation of treatment, sebum output is restored to a level seen before treatment. Despite this return to the pre-treatment sebum level, many patients remain clear of acne. Thus, a temporary effect on sebaceous glands may be sufficient to cause a long-term or even permanent acne clearance. Whether such an effect can be brought about by a photothermal laser treatment targeting the sebaceous glands in the upper dermis is examined in this work. Here, a laser treatment is presented which is shown to thermally alter the sebaceous glands while preserving the epidermis. Results of modeling calculations, histology studies, and human clinical studies are presented.

MATERIALS AND METHODS

Choice of Wavelength

Skin can be divided into three layers: epidermis (up to a depth of 60–100 μm), the dermis (up to a depth of about 2–5 mm), and subcutaneous fat, just below the dermis. Within skin, sebaceous glands are located at depths from about 200–1,000 μm [7] below the stratum corneum. Since the goal of the sub-surface treatment is to spare the epidermis and thermally injure the dermis where the sebaceous gland structure including the infundibulum resides, the desired penetration depth of light in skin is about 400 μm . From Monte Carlo simulations discussed later, at the wavelength of 1,450 nm, the penetration depth is 435 μm with water being the principal absorber in skin. Thus, this wavelength of 1,450 nm was chosen to produce an injury zone in the dermal region where sebaceous glands are located.

Choice of Cooling

Cutaneous laser treatments have been combined with various cooling methods that can be classified broadly into cryogen spray cooling, cold air-cooling, and contact cooling. Cryogen spray cooling, with its precise control of spray durations, can selectively cool the epidermis while leaving the temperature of the dermis unchanged [8]. Hence, cryogen spray cooling was used in this application. In this method, cryogen spurts were applied to the skin surface for a period on the order of 10 milliseconds. The cryogen used was tetrafluoroethane, an EPA approved refrigerant and FDA approved propellant with a boiling point of -26°C at atmospheric pressure.

Treatment Device

The laser device (Candela Corporation, Wayland, MA) employed a combination of diode laser light at 1,450 nm and an integrated dynamic cooling device (DCDTM) that provides cryogen spray cooling. The cryogen cooling allowed preservation of the epidermis, thus minimizing side effects. The radiant exposure range was from 14 to 22 J/cm^2 with

total laser duration in the range of 160–200 milliseconds that was divided into four pulses of equal durations, interspersed with three cryogen sprays. The scheme of interspersing four laser sub-pulses with cryogen pulses was implemented so as to avoid thermal damage to the epidermis. The irradiance ranged from 87 to 110 W/cm^2 . In addition, there was a pre-laser spray and a post-laser spray. All sprays were adjustable for precise durations. The timing diagram is shown in Figure 1 which shows a pre-spray duration of 15 milliseconds, three intermediate sprays of 15 milliseconds duration each, and a post-laser spray of 20 milliseconds duration. The laser light from the device was coupled into an optical fiber. Optics at the end of the fiber produced a homogeneous collimated 4-mm diameter circular beam on skin.

Monte Carlo Simulations of Light Transport and Heat Transfer Calculations

Light transport and heat transfer calculations were performed to serve as a guide in optimizing the treatment parameters. The results that were obtained were not expected to be exact but were useful in understanding the temperature distribution and thermal injury for various treatment parameters and for optimization of the same.

In skin, the primary absorber at this wavelength is water and it is assumed that the water content does not vary as a function of depth. A single layer model with constant absorption and scattering properties is used in skin. The absorption coefficient of water is dependent on temperature. In an extreme case, the temperature of the skin upon treatment can increase from 30°C to a maximum of 90°C . The change in μ_a of water with 1°C temperature increase has been reported to be $-0.01475 \text{ cm}^{-1}/^\circ\text{C}$ [9]. A temperature change of 60°C corresponds to a change in absorption coefficient of -0.885 cm^{-1} . If skin is 70% water, the change in absorption coefficient of skin would be -0.6195 cm^{-1} . A change of 0.6195 cm^{-1} in the skin absorption coefficient of 20 cm^{-1} is small and hence the dependence of absorption coefficient on temperature is neglected. The absorption properties [9] and scattering properties [10] at 1,450 nm wavelength as given in Table 1 were used as input for the simulations. A circular homogeneous collimated 4-mm diameter beam was incident on the tissue surface.

The tissue volume was discretized into a three-dimensional grid with 41, 41, and 1,001 grid points in the x, y, and z directions, respectively, where z-direction is perpendicular to skin surface. The separation between grid points was 0.025, 0.025, and 0.0025 cm in x, y, and z directions,

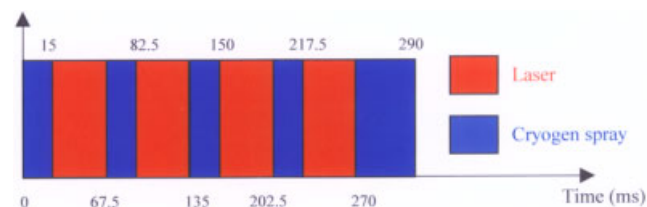


Fig. 1. A timing diagram showing alternate cryogen spray and laser pulses used per treatment shot.

TABLE 1. Optical Properties Used in the Monte Carlo Model for Calculation of Light Fluence Rate Distribution

Component	Refractive Index, n	Absorption coefficient, μ_a	Scattering coefficient, μ_s	Anisotropy factor, g
Air	1	0	0	0
Skin	1.37	20 cm^{-1}	120 cm^{-1}	0.9

respectively. Monte Carlo simulations were performed to calculate light fluence rate at all grid points within the tissue using the MCML software, given the optical absorption and scattering properties of skin [11,12].

In a second step, heat transfer calculations were performed by solving the heat conduction equation, as given in Eq. (1), numerically by a finite-difference method.

$$\frac{\partial T(x, y, z, t)}{\partial t} = \frac{k}{\rho C_p} \nabla^2 T(x, y, z, t) + \frac{\mu_a \phi(x, y, z, t)}{\rho C_p}, \quad (1)$$

$T(x, y, z, t)$ is the temperature at location (x, y, z) and time t ; k , ρ , and C_p are the thermal conductivity, density, and specific heat of skin, respectively. The last term on the right represents heat generation within tissue due to absorption of light in which $\phi(x, y, z, t)$ is the fluence rate. The boundary condition at the top surface (perpendicular to the z -axis) is described by the convective boundary condition as described by Eq. (2).

$$-k \frac{\partial T}{\partial z} = h_{\text{coolant}} (T_{\text{tissue-surface}} - T_{\text{coolant}}). \quad (2)$$

In the above equation, h is the convective heat transfer coefficient for either air-skin or cryogen-skin interface. T_{coolant} is the temperature of either cryogen or air that is in contact with the tissue. The air-skin heat transfer coefficient and air temperature are used for the top surface except on the treatment spot where the respective values for cryogen-skin are used during the time period when cryogen spray is incident on skin. The value of the cryogen-skin heat transfer coefficient has been reported as high as $40,000 \text{ W/m}^2\text{K}$ [13] and as low as $2,400 \text{ W/m}^2\text{K}$ [14]. An intermediate value of $4,000 \text{ W/m}^2\text{K}$ has been reported by Pikkula and we used this value [15]. Torres et al. [14] reported the cryogen temperature to be -44°C and we used this value. The values of air-skin heat transfer coefficient and air temperature chosen were $50 \text{ W/m}^2\text{K}$ and 30°C , respectively. The parameters used in the heat transfer calculations are provided in Table 2. For the finite difference heat transfer calculations, the tissue volume was discretized into a three-dimensional grid with 21, 21, and 101 grid points in the x , y , and z directions, respectively. The separation between grid points was 0.05, 0.05, and 0.005 cm in

x , y , and z directions, respectively. The time increment was chosen as 3 milliseconds.

The kinetic thermal damage model relates the temperature-time history of tissue to the thermal damage. The thermal damage measure, Ω , is traditionally defined as the logarithm of the ratio of the original concentration of native tissue, $C(0)$, to the remaining native state tissue, $C(t)$, and by using an Arrhenius-type kinetic model, it is given at a time t by Eq. (3).

$$\Omega(t) = \ln\{C(0)/C(t)\} = \int_0^t \{A \exp(-E_a/RT(\tau))\} d\tau \quad (3)$$

where A is a pre-exponential factor, E_a is the activation energy, R is the universal gas constant, and $T(\tau)$ is the thermal history as a function of time τ [16]. The parameters A and E_a are typically determined by fitting experimental measurements of damaged and undamaged tissue concentrations as a function of time and temperature. This behavior is to be expected from the exponential nature of the function. A set of parameters, $E_a = 6.28 \times 10^5 \text{ J/mole}$ and $A = 3.1 \times 10^{98} \text{ sec}^{-1}$ has been reported [16]. The damage was calculated as a function of depth in skin through the center of the treated spot by numerically evaluating the integral given in Eq. (3) with the above parameters and the calculated temperature evolution with time.

Ex Vivo Human Skin Histology

A human skin sample was obtained from an elective breast reduction at the University of Massachusetts Memorial Hospital, Worcester, MA. The sample was transported at 4°C and used in the experiments within 8 hours. During the experiment, the sample was placed on a warm metal plate, the temperature of which was maintained at 32°C by immersing part of it in a temperature-controlled water bath. Treatments were performed on different spots with a 4-mm diameter spot with various combinations of spray and radiant exposures. Biopsies with a 3-mm punch were taken and fixed in a 10% buffered formalin solution within 20 minutes after the treatment. The samples were processed and stained by hematoxylin and eosin (H&E) stain and examined microscopically.

TABLE 2. Values of Parameters Used in the Heat Transfer Calculations

Laser radiant exposure	Spot size	Laser pulse duration	Cryogen temperature	Pre-laser spray duration	Intermediate spray duration (split in 3)	Post-laser spray duration	Thermal diffusivity of tissue, $k/\rho C_p$	Cryogen-skin heat transfer coefficient
16 J/cm^2	4 mm	210 ms	-44°C	15 ms	45 ms	20 ms	$8 \times 10^{-4} \text{ cm}^2/\text{sec}$	$4,000 \text{ W/m}^2\text{K}$

Rabbit Ear Histology Study

The rabbit ear model has been developed by Kligman and Mills [17]. The rabbit ear histological study was intended to test the following hypothesis: Thermal injury to sebaceous glands residing within the dermis is caused by the laser whereas the thermal injury to the epidermis is prevented by the DCD cryogen spray. The thermal injury to the epidermis, the dermis, sebaceous glands and associated structures in the dermal region was evaluated after treatment with the test laser device in a rabbit ear model with a wide range of treatment parameters.

The study was conducted at Primedica Corporation, Worcester, MA. Institutional Animal Care and Use Committees (IACUC) approval was obtained prior to the animal study. The procedures and animal husbandry was performed as described in the "Guide for the Care and Use of Laboratory Animals," National Research Council, revised 1996 and/or in accordance with the standard operating procedures of Primedica. The 19 New Zealand white rabbits in this study, aged 6–9 months, underwent procedures as indicated in Table 3. Six treatment sites per ear were marked by tattoo ink on the ventral aspects of each ear. Hair was clipped from the ears prior to tattooing and treatment. Rabbits were tranquilized with a subcutaneous injection of medetomidine prior to tattooing, laser treatment, punch biopsy collection and as necessary to facilitate handling. A single treatment parameter set was used on each ear on six treatment spots. On day 1, laser treatment was applied within the boundaries of each treatment site with a 4-mm diameter spot. Within an hour after treatment, tissue samples from two adjacent sites per ear for one treatment parameter set and a single untreated control site were obtained by a 3-mm punch biopsy. Two more punch biopsies of treated sites of each ear were also collected on day 3. The final treatment sites and control tissue were collected at necropsy on day 7. Prior to necropsy, euthanasia was performed by deep anesthesia with IV sodium pentobarbital, followed by exsanguination. Tissue samples from the treated and control sites were evaluated histopathologically. Several radiant exposures and DCD settings were evaluated.

Human Clinical Study

The objective of this study was to evaluate the effectiveness of the 1,450 nm laser for the treatment of acne. Twenty seven subjects were enrolled in the study conducted at the Naval Medical Center in San Diego, CA. Volunteers with acne on bilateral areas of the upper back were enrolled. At baseline, the acne severity was similar

on both sides of the back. Institutional Review Board approval was obtained prior to initiation of the study and informed consent was obtained from each of the patients prior to enrollment.

Bilateral areas of the treated and control sites were mapped on a transparent paper to track the location of lesions and ensure the accuracy of site selection and lesion counts at all time points. The selection of treated and control sides was randomized. The treatment area received laser and cryogen, while the control area received only cryogen spray. The areas of treated and control sites on the back were up to approximately 36 cm² each. Four treatments separated by a period of 3 weeks were administered to the same treated area. The treatment was performed on the entire selected area and not necessarily on lesions only.

After the first treatment, patients were seen for a 1-day and a 1-week follow-up. For subsequent treatments, they were seen every 3 weeks for follow-ups and treatments until each completed a total of four treatments. After the fourth treatment, patients were seen for follow-up visits at 6, 12, and 24 weeks. Photographs of the treated and control sides were taken before the initial treatment at every treatment or follow-up visit. The radiant exposure was chosen by the clinical investigator so as to be lower than the radiant exposure that caused epidermal whitening. Radiant exposure values ranged between 14 and 22 J/cm²; the cooling parameters for each subject were kept the same or varied slightly. The average radiant exposure was 18 J/cm².

During all treatments and follow-up visits, the physicians and staff recorded and maintained records of all patients describing clinical observations associated with the treatments, including lesion counts, acne severity, as well as before and after photographs. Lesion counts included all non-inflammatory and inflammatory lesions. Biopsies of treatment sites were obtained immediately after treatment in four subjects. Additional biopsies were obtained at 6, 12, or 24-week follow-ups. The biopsy samples taken immediately after treatment were fixed in formalin and examined microscopically after H&E staining. Histological analyses of the treatment effects on both the skin and the sebaceous glands were performed.

Clinical observations of the treated and control sides were graded and recorded. These observations included new or recurrent lesion counts, acne severity, erythema, edema, blistering, abnormal pigmentation (hyper- or hypo-), and scarring. The assessment of the above observations was performed at all time points on a scale of 0–3 (0, absent; 1, mild; 2, moderate; and 3, severe).

TABLE 3. Rabbit Ear Histology Study Design Table

Number of animals	Right ear	Left ear	Laser treatment	Punch biopsy	Necropsy
19	6 treatment sites/animal	6 treatment sites/animal	Day 1, each treatment site	Day 1 and 3	Day 7

Day 1 punch biopsy = just after treatment (within 1 hour).

In the data analysis, the mean lesion count and the standard deviation at baseline and at different follow-up time points were calculated. Student *t*-test (paired samples) was performed comparing the lesion counts at the baseline with that at different follow-up time points for both the treated and control sides.

RESULTS

Monte Carlo Simulations of Light Transport and Heat Transfer Calculations

The results of the Monte Carlo simulations yielded the penetration depth, defined as the depth at which the fluence rate reaches (1/e), i.e., 36.8% of the fluence rate at the surface, as 439 μm. If scattering effects were absent, the penetration depth, according to Beer law, is 1/μ_a or 1/20 cm⁻¹ or 500 μm. Thus, scattering effects reduce the penetration depth to 439 μm. The results of one representative calculation are discussed. Laser energy of 2.01 J with a 4-mm circular spot that corresponds to a radiant exposure of 16 J/cm² was used. A cooling scheme that provides a pre-laser spray of 15 milliseconds, three intermediate sprays of 15 milliseconds each, and a final post-laser spray of 20 milliseconds was employed. This scheme was expected to lead to epidermal preservation. The total laser time of 210 milliseconds was divided into four pulses of equal durations and equal energies. The evolution of spatial temperature profiles with time was calculated.

Figure 2 shows a color plot of calculated temperature versus time and depth. Different colors represent different levels of temperature. The repeated cryogen sprays cooled the epidermis whereas laser caused heating of the upper dermis. The peak temperature was calculated to be 88.8°C at the end of the last laser sub-pulse at a depth of 150 μm. Figure 3 shows the damage profile predicted by the kinetic thermal damage model on a log scale as a function of depth along the center of the treatment spot. The magnitude of

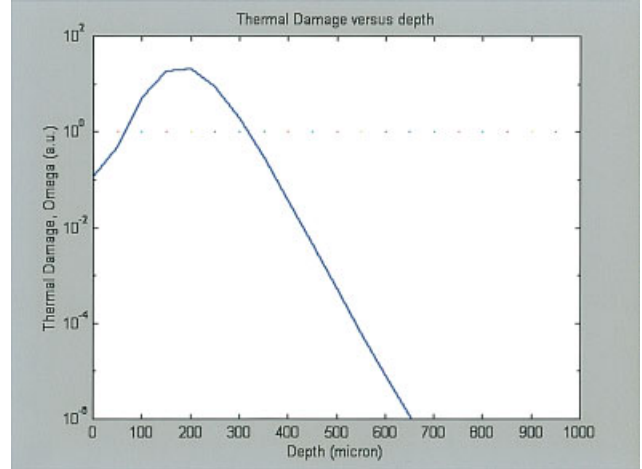


Fig. 3. A plot of thermal damage versus depth in skin.

the damage can be increased or decreased by adjusting the laser radiant exposure.

Ex Vivo Human Skin Histology

Figure 4 shows a histological section of skin after treatment with radiant exposure of 20.6 J/cm², pre-laser spray of 10 milliseconds, intermediate spray consisting of three sprays of 10 milliseconds each, and a post-laser spray of 20 milliseconds. It shows that the epidermis is preserved whereas the upper dermis is darker and coagulated indicating thermal damage. The typical laser radiant exposure values used in non-ablative treatment of subjects as discussed later are lower than the value used in demonstrating the histology and hence the treatments created a milder thermal injury.

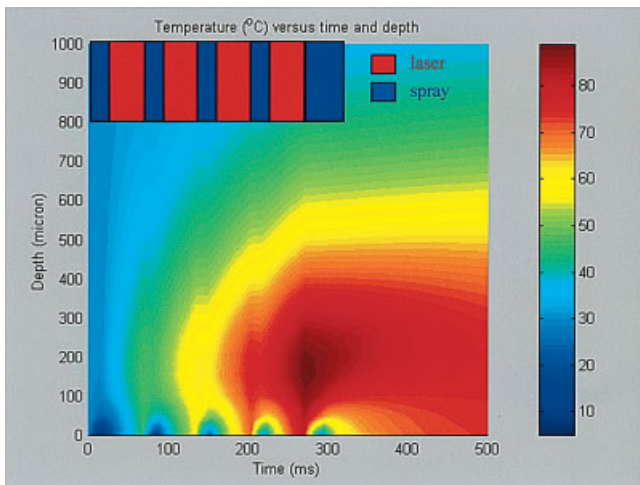


Fig. 2. A color plot of calculated temperature versus time and depth. Five cryogen pulses result in epidermal cooling. Thermal heating of the upper dermis is achieved.

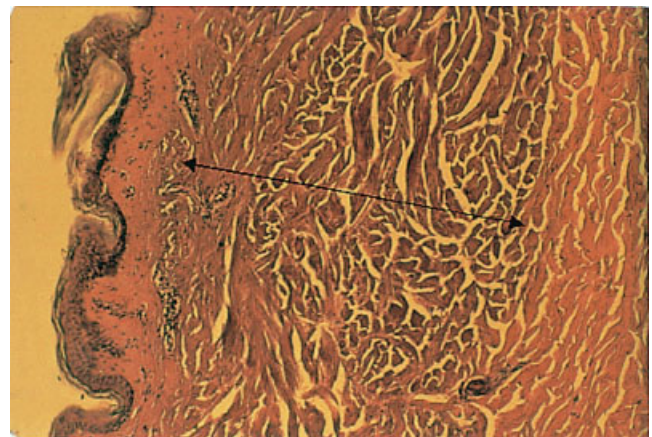


Fig. 4. Histological section through the treatment spot of *ex vivo* human skin immediately after treatment processed with H&E staining. The arrow indicates the zone of thermal damage. Note epidermal preservation and thermal damage within the upper dermis.

Rabbit Ear Histology

Sebaceous necrosis with minimal epidermal damage was seen for several parameter sets on the treated side. No changes were seen on the control side. Figure 5 shows a photograph of the biopsy section at day 1, after a radiant exposure of 15 J/cm^2 and no DCD. Full thickness necrosis is seen. The dermis and the associated sebaceous glands are completely destroyed. Also, the epidermis is also destroyed since no cooling was used. Figure 6 shows a photograph of the slide at day 1 after treatment with 24 J/cm^2 and a DCD consisting of a pre-spray of 10 milliseconds, three intermediate sprays of 13.3 milliseconds each, and a post-spray of 20 milliseconds; see Figure 1 for the timing diagram of sprays. The epidermis was mostly preserved whereas the dermis was damaged; some epidermal separation was noted however. Three lobes of sebaceous glands were thermally damaged. Both tinctorial changes and pyknotic nuclei were seen in the damaged sebaceous glands. A close up of the damaged sebaceous gland is shown in Figure 7. Similar epidermal preservation and damage to the dermis and sebaceous glands was seen at day 3 for the parameter sets of 24 J/cm^2 and DCD consisting of a pre-spray of 10 milliseconds, three intermediate sprays of 10 milliseconds each, and post-spray of 20 milliseconds as shown in Figure 8. A close-up photograph of damaged sebaceous glands is shown in Figure 9. At day 7, several sebaceous glands were found to be present and undamaged under the histological examination for most of the parameter sets.

Human Clinical Study

Clinical efficacy: acne improvement. The mean lesion count and the standard deviation at baseline and at different follow-up time points are given in Table 4. The p -values from a Student t -test (paired samples) comparing the lesion counts at baseline with those at different follow-up time points for both the treated and control sides are also given. For the 6, 12, and 24-week follow-up time points, there is a mean reduction of five or more lesions on

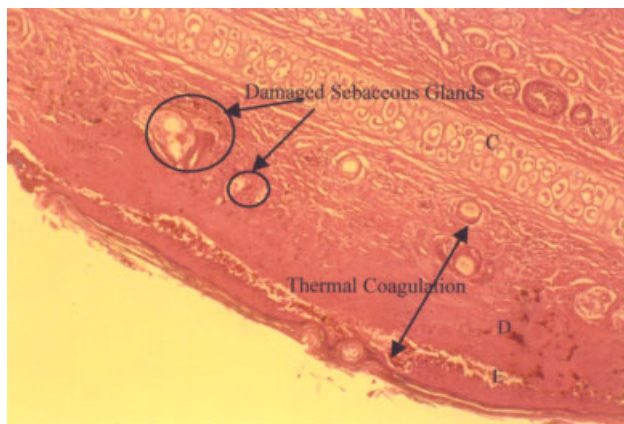


Fig. 5. Histology of rabbit ear after treatment with 15 J/cm^2 and no DCD at day 1. 'E', epidermis; 'D', dermis; and 'C', cartilage in this and all following figures.

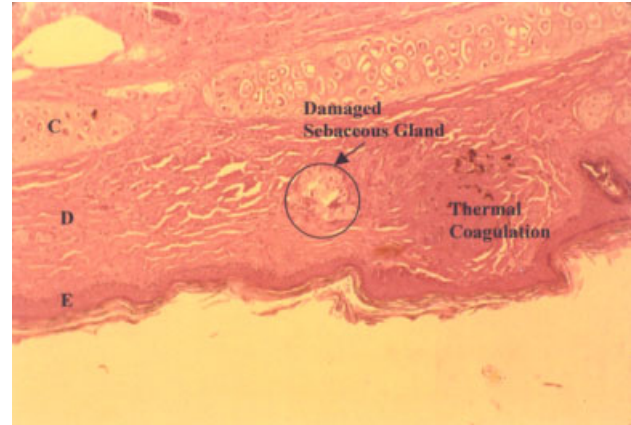


Fig. 6. Histology of rabbit ear with 24 J/cm^2 and DCD consisting of a pre-spray of 10 milliseconds, three intermediate sprays of 13.3 milliseconds each, and a post-spray of 20 milliseconds at day 1.

the treated side and a small change on the control side. A statistically and clinically significant reduction ($p < 0.01$) in lesion counts was seen on the treated side. While the number of subjects at different follow-up times varied, for all 15 subjects completing their 24-week follow-up, no acne lesions were seen on the treated areas of 14 subjects.

Figure 10 is a photograph of the treated side on a subject's back 3 weeks after the second treatment. Four marks delineate the treatment area within which clearance of lesions is seen while lesions are seen outside the treated area. Figure 11 shows a photograph of the control side of the same subject's back at the same time point. Several lesions are seen on the control side.

Safety and side effects. There were no unusual side effects or adverse reactions. In brief, the most common clinical effect seen in subjects as a response to the treatments was erythema, which was expected. Erythema and

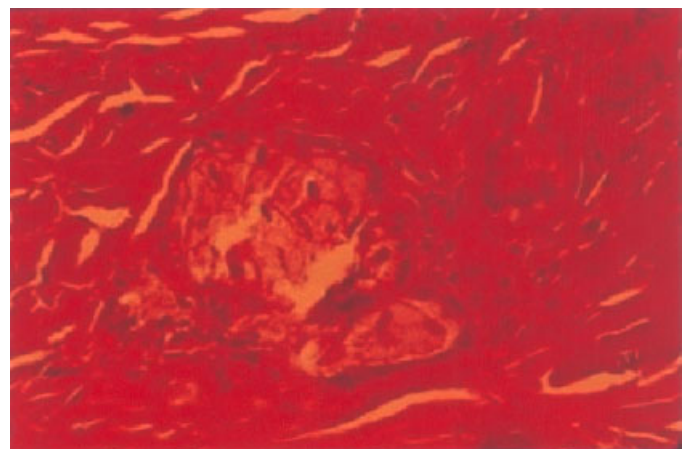


Fig. 7. A close-up of the damaged sebaceous glands showed in Figure 6.

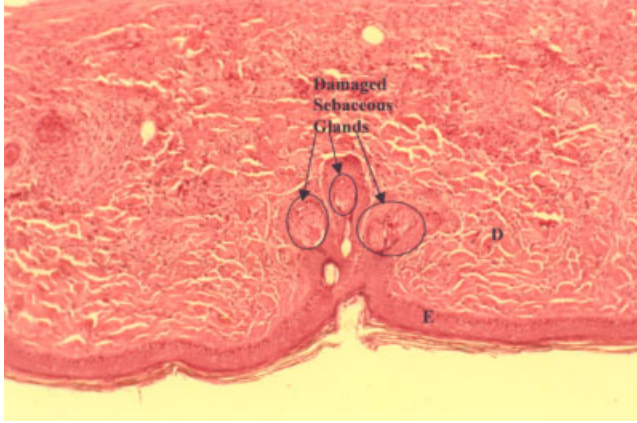


Fig. 8. Histology of rabbit ear after treatment with 24 J/cm² and DCD consisting of a pre-spray of 10 milliseconds, three intermediate sprays of 10 milliseconds each, and post-spray of 20 milliseconds at day 3.

edema had resolved by the next follow-up observation. Three out of twenty-seven subjects showed hyperpigmentation at some time during the treatment regimen. Hyperpigmentation was graded “severe” for one subject at one time point; the other two were classified as “mild.” Hyperpigmentation uniformly resolved and was absent for all subjects at the 6, 12, and 24-week follow-ups after the fourth treatment. No signs of purpura or scarring were evident in any subject at any time point.

Histological changes after treatment. The density of sebaceous glands on the back skin is not high and only one of the biopsy samples taken immediately after treatment yielded sebaceous glands. In this biopsy sample obtained after treatment with 17.2 J/cm² and DCD with pre-spray of 10 milliseconds, three intermediate sprays of 10 milliseconds each, and a post-spray of 20 milliseconds, a rupture of the pilosebaceous unit with thermal coagulation of the sebaceous lobule and follicle was noted as seen in Figure 12. The overlying epidermis was unaltered. Long term biopsies taken at 2 and 6 months after the treatment

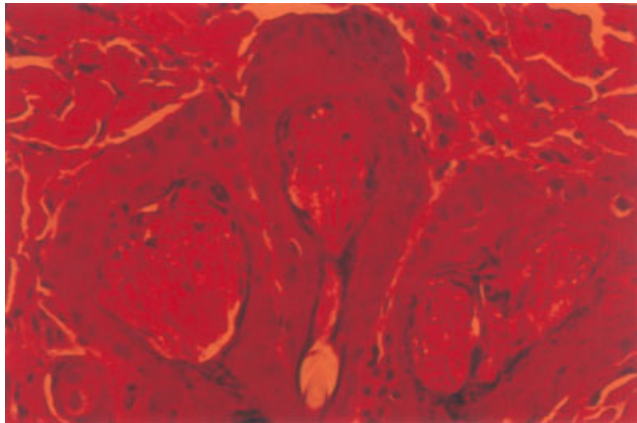


Fig. 9. A close-up of the damaged sebaceous glands shown in Figure 8.

TABLE 4. Results of Student *t*-Test (Paired Samples) Comparing the Lesion Count Between Follow-Up and Baseline for the Treated and Control Sides

Follow-up time-point	N	Treatment		<i>p</i> -value	Control		<i>p</i> -value
		Mean lesion count (standard deviation) at baseline	Mean lesion count (standard deviation) at follow-up		Mean lesion count (standard deviation) at baseline	Mean lesion count (standard deviation) at follow-up	
3 weeks post Tx no. 1	27	7.22 (3.59)	2.67 (2.24)	1.09 × 10 ⁻¹⁰	5.81 (2.37)	5.93 (3.05)	0.75
3 weeks post Tx no. 2	23	7.13 (3.49)	1.04 (1.66)	2.19 × 10 ⁻¹⁰	5.70 (2.40)	5.48 (2.04)	0.55
3 weeks post Tx no. 3	22	7.18 (3.57)	0.68 (1.86)	2.34 × 10 ⁻⁹	5.77 (2.43)	5.68 (2.23)	0.78
6 weeks post Tx no. 4	20	6.80 (3.12)	0.15 (0.67)	1.56 × 10 ⁻⁸	5.65 (2.43)	4.95 (1.88)	0.05
12 weeks post Tx no. 4	17	6.94 (3.36)	0.12 (0.33)	1.64 × 10 ⁻⁷	5.53 (2.58)	5.06 (2.16)	0.24
24 weeks post Tx no. 4	15	5.67 (1.29)	0.13 (0.52)	8.22 × 10 ⁻¹¹	5.00 (2.14)	4.73 (1.98)	0.68

The mean difference, standard deviation, and the *p*-value are presented at each follow-up time point.

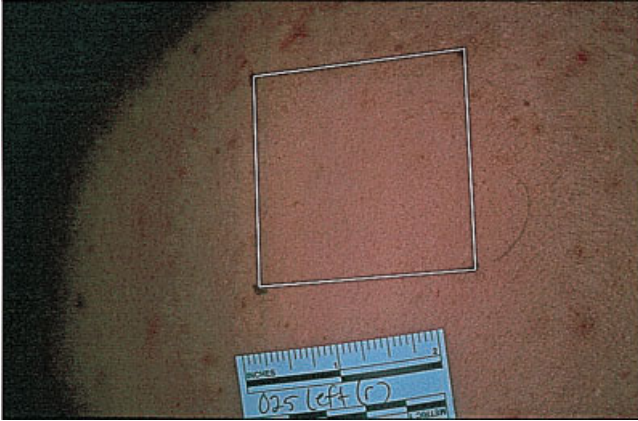


Fig. 10. Photograph of the treated area at 3 weeks after the second treatment. Lesions clearance is seen.

on the back and face with similar treatment parameters showed sebaceous glands and associated ductal structures that were unaltered from their pre-treatment (control) counterparts. Therefore, on routine microscopy, there appeared to be no long-term alteration in adnexal structure architecture. The epidermis and the follicular structures also appeared normal.

DISCUSSION AND CONCLUSIONS

Various light-based therapies are under development for treatment of acne. Reduction in acne lesion count upon exposure to blue, red, violet, and ultra-violet light have been reported [18–22]. The mechanism of treatment with blue light is believed to be absorption by endogenous porphyrins produced by *P. acnes* and subsequent phototoxic effect on *P. acnes* to cause a beneficial effect in acne symptoms [18]. These therapies do not target sebaceous glands as such and long-term remission is not proven and may not be possible since repopulation by *P. acnes* is likely to occur after cessation of treatment. Hongcharu et al. [23] have reported treatment of acne with aminolevulinic acid

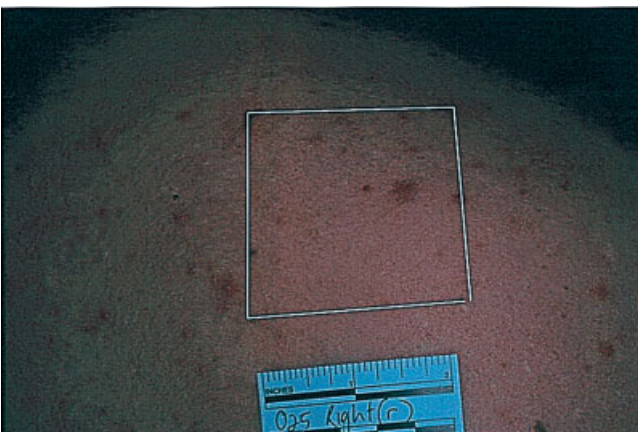


Fig. 11. Photograph of the control area at 3 weeks after the second treatment. Lesions are still present.

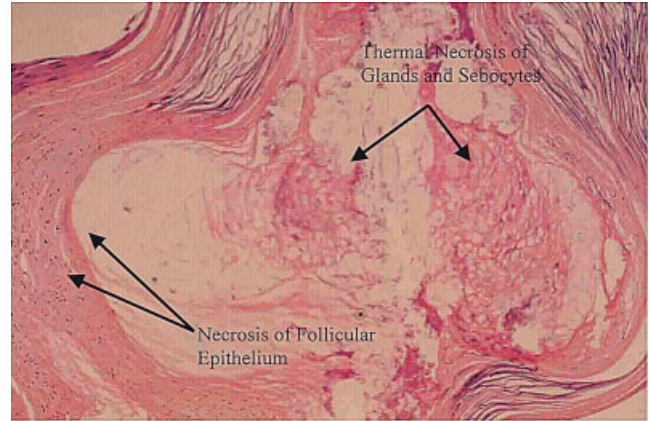


Fig. 12. Histology of treated human back skin after treatment; a close-up of a sebaceous gland. A complete rupture of the pilosebaceous unit with thermal coagulation of the entire sebaceous lobule and follicle is seen.

(ALA)-photodynamic therapy (PDT). ALA was applied topically and the skin was irradiated with light in the 550–700 nm wavelength range. Clinically and statistically significant clearance of inflammatory acne for 10 weeks after a single treatment and at least 20 weeks after multiple treatments was observed. However, transient hyperpigmentation, superficial exfoliation, and crusting were observed. They concluded that topical ALA plus red light is an effective treatment for acne vulgaris, although associated with significant side effects. In another study on ALA-PDT [24], all patients had apparent improvement of facial appearance and reduction of new acne lesions at 1, 3, and 6 months following PDT treatment. The adverse effects were discomfort, burning, and stinging during irradiation, edematous erythema for 3 days after PDT, epidermal exfoliation from the 4th to the 10th day, irritation and hypersensitivity to physical stimulation for 10 days after PDT, and pigmentation or erythema after epidermal exfoliation. In summary, ALA-PDT may be an effective treatment but is associated with side effects.

In this article, a device combining a diode laser at 1,450 nm wavelength and cryogen cooling has been studied for non-ablative treatment of acne vulgaris. Monte Carlo modeling and heat transfer calculations predict that the combination of DCD cooling and 1,450 nm laser can be used to achieve thermal damage that is peaked around a depth of 150–200 μm while minimizing the damage in the epidermis and in the deeper dermis. Only qualitative and not quantitative comparisons can be made between the modeling calculations and the experiments due to the many approximations implicit in the model calculations. Histological examination of *ex vivo* human skin showed that the concept of achieving thermal injury to the upper dermis while preserving the epidermis is feasible. Rabbit ear was used as a model to study the histological effects of the irradiation with laser and cooling with DCD. Various treatment parameters were used. Histological analysis at day 1 and 3 with certain treatment parameters showed damage

to the dermis and thermal alteration of sebaceous glands located within the dermis while the epidermis was preserved. Histological examination of biopsies taken at day 7 indicated that sebaceous glands were intact or had recovered from initial injury. Biopsies and histology of *ex vivo* human skin showed that it is possible to achieve heating of the dermal region containing the sebaceous glands while preserving the epidermis. Immediate as well as 3- and 7-day histological response to treatment was studied on the rabbit ears. This showed thermal alteration of the sebaceous glands immediately and at 3 days; the sebaceous glands do not show pronounced histological effect at the 7-day time point.

A human clinical study for the treatment of acne vulgaris was conducted on backs of males with a 1,450 nm laser combined with cryogen spray cooling. A reduction in lesion count was seen immediately after first treatment. A statistically and clinically significant reduction in lesion counts was seen on the treated side compared to the control side at the 6, 12, and 24-week follow-ups after the fourth treatment. Longer-term follow-ups will be performed to see if these results persist. Side effects included transitory erythema and edema. Although four treatments were used in this study, reduction in acne lesions was seen after a single treatment. Thus, lower number of treatments may suffice. Determination of optimum number of treatments and interval between treatments is being done. Histological analysis of biopsies obtained immediately after treatment indicated an alteration in sebaceous glands structure. Long term biopsies after the treatment on the back showed sebaceous glands and associated ductal structures that were unaltered from their pre-treatment (control) counterparts. The reduction in acne lesion count is likely due to a slight functional impairment of the glands secondary to mild thermal damage created at the time of irradiation. Accutane, an effective treatment of acne, also has a temporary effect on sebaceous glands. Further studies on histological and clinical effects of this treatment on the facial acne in humans are in progress. This treatment may have a secondary effect on sebum production rate and *P. acnes* population, both of which are associated with acne. The effect of the laser treatment on these two is being evaluated in ongoing studies.

ACKNOWLEDGMENTS

The rabbit ear histology study was supported by the National Institutes of Health Grant Number 1R43AR4-6938-01. The authors thank Dr. Elliot Lach for providing the skin samples used in the *ex vivo* human skin study.

REFERENCES

- Bergfeld WF, Odom RB. New perspectives on acne. *Clinician* 1994;12:3-29.
- Kellett SC, Gawkrödger DJ. The psychological and emotional impact of acne and the effect of treatment with isotretinoin. *Br J Dermatol* 1999;140:273-282.
- Sykes NL, Webster GJ. Acne: A review of optimum treatment. *Drugs* 1994;48:59-70.
- Eady EA. Bacterial resistance in acne. *Dermatology* 1998;196:59-66.
- Turkington CA, Dover JS. *Skin Deep: An A-Z of Skin Disorders, Treatment and Health*. New York: Facts on File, Inc; 1996. p 8.
- Plewig G, Kligman AM. *Acne and Rosacea*, 2nd edn. Berlin: Springer-Verlag; 1993. p 711.
- Montagna W, Kligman AM, Carlisle KS. Estimation from histology photographs in Atlas of Normal Human Skin. New York: Springer-Verlag; 1992.
- Anvari B, Tanenbaum BS, Milner TE, Kimel S, Svaasand LO, Nelson JS. A theoretical study of the thermal response of skin to cryogen spray cooling and pulsed laser irradiation: Implications for treatment of port wine stain birthmarks. *Phys Med Biol* 1995;40:1451-1465. [published erratum appears in *Phys Med Biol* 1996; 41:1245.]
- Gardner CM. Absorption coefficient of water. Personal Communication, Brookline, MA, 5/6/1998.
- Lask GP, Lee PK, Seyfzadeh M, Nelson JS, Milner TE, Anvari B, Dave D, Geronemus RG, Bernstein LJ, Mittelman H, Ridener LA, Coulson WF, Sand B, Baumgardner J, Hennings DR, Menefee RF, Berry M. Nonablative laser treatment of facial rhytides. *Proc SPIE* 1997;2970:338-349.
- Jacques SL, Wang LH. Monte Carlo modeling of light transport in tissue. Optical thermal response of laser irradiated tissue. Chapter 4. New York: Plenum Press; 1995. 73-100.
- Wang LH, Jacques SL, Zheng LQ. MCML—Monte Carlo modeling of photon transport in multi-layered tissues. *Comput Methods Programs Biomed* 1995;47:131.
- Anvari B, Milner TE, Tanenbaum BS, Nelson JS. A comparative study of human skin thermal response to sapphire contact and cryogen spray cooling. *IEEE Trans Biomed Eng* 1998;45:934-941.
- Torres JH, Nelson JS, Tanenbaum BS, Milner T, Goodman DM, Anvari B. Estimation of internal skin temperatures in response to cryogen spray cooling: Implications for laser Therapy of port wine stains. *IEEE J Selected Top Quantum Electron* 1999;5:1058-1066.
- Pikkula B. Heat transfer coefficient at the skin-cryogen interface. Personal Communication, Houston, TX, 12/13/2001.
- Pearce J, Thomsen S. Rate process analysis of thermal damage. Chapter 17. In: Welch AJ, van Gemert MJC, editors. *Optical-thermal response of laser-irradiated tissue*. New York: Plenum Press; 1995. pp 160-162.
- Kligman AM, Mills OH. Acne cosmetica. *Arch Dermatol* 1972;106:843.
- Shalita AA, Harth Y, Elman M, Slatkine M, Talpalariu G, Rosenberg Y, Korman A, Klein A. Acne phototherapy using u.v. free high intensity narrow band blue light—3 center clinical study. *Proc SPIE* 2001;4244:61-73.
- Cunliffe WJ, Goulden V. Phototherapy and acne vulgaris. *Br J Dermatol* 2000;142:855-856.
- Papageorgiou P, Katsambas A, Chu A. Phototherapy with blue (415 nm) and red (660 nm) light in the treatment of acne vulgaris. *Br J Dermatol* 2000;142:973-978.
- Konig K, Ruck A, Schneckenburger H. Fluorescence detection and photodynamic activity of endogenous protoporphyrin in human skin. *Opt Eng* 1992;31:1470-1474.
- Meffert H, Scherf HP, Sonnichsen N. Treatment of acne vulgaris with visible light. *Dermatol Monatsschr* 1987;173:678-679.
- Hongcharu W, Taylor CR, Chang Y, Aghassi D, Suthamjariya K, Anderson RR. Topical ALA-photodynamic therapy for the treatment of acne vulgaris. *J Invest Dermatol* 2000;115:183-192.
- Itoh Y, Ninomiya Y, Tajima S, Ishibashi A. Photodynamic therapy of acne vulgaris with topical delta-aminolaevulinic acid and incoherent light in Japanese patients. *Br J Dermatol* 2001;144:575-579.